Resonant frequency analysis of a Lamé-mode resonator on a quartz plate by the finite-difference time-domain method using the staggered grid with the collocated grid points of velocities

Takashi Yasui[*,1], Koji Hasegawa[2], and Koichi Hirayama[1]

[1] *Kitami Institute of Technology, Kitami, Hokkaido 090-8507, Japan*

[2] *Muroran Institute of Technology, Muroran, Hokkaido 050-8585, Japan*

The finite-difference time-domain (FD-TD) method using a staggered grid with the collocated grid points of velocities (SGCV) was formulated for elastic waves propagating in anisotropic solids and for a rectangular SGCV. Resonant frequency analysis of Lamé-mode resonators on a quartz plate was carried out to confirm the accuracy and validity of the proposed method. The resonant frequencies for the fundamental and higher-order Lamé-modes calculated by the proposed method agreed very well with their theoretical values.

The finite-difference time-domain (FD-TD) method is a powerful and attractive tool for modeling the propagation and scattering of acoustic[1–8)] and elastic[9–19)] waves. Discretization of two first-order partial differential equations with finite difference approximations results in a staggered grid (SG),[9)] a rotated SG,[11)] a diagonally SG,[13)] a Lebedev grid,[14)] and an SG with collocated grid points of velocities (SGCV).[17–20)]

To model elastic wave devices by the FD-TD method, implementation of boundary conditions on planar free surfaces is necessary. For the conventional SG, a rather complicated scheme such as the stress-imaging technique[10)] is required, since tangential components of stress are on the free surfaces.

The SGCV was presented to realize a much simpler implementation of boundary conditions for the FD-TD method.[17)] The resonant frequency analyses of the fundamental and higher-order modes of Lamé-mode resonators on an isotropic solid by the FD-TD method with a square SGCV were carried out to demonstrate the simply imposed boundary conditions on free surfaces.[18,19)]

Because many important materials for elastic wave devices are anisotropic, the FD-TD method with an SGCV should be extended to anisotropic materials. Although a resonant frequency analysis for a Lamé-mode resonator based on an anisotropic plate

[*]E-mail: yasui@mail.kitami-it.ac.jp

was carried out,[20] it was applied to only the fundamental mode. In addition, the accuracy of the SGCV for anisotropic materials has not been investigated in detail.

In this study, the FD-TD method with a rectangular SGCV, which enables us to model Lamé-mode resonators with arbitrary aspect ratio, is formulated for elastic waves propagating in anisotropic materials. To show the validity of the proposed method, the resonant frequencies of the fundamental and higher-order modes of Lamé-mode resonators on a quartz plate are evaluated. The convergence of resonant frequencies is also investigated to show the accuracy of the proposed method.

Newton's equation of motion and Hooke's law are respectively represented in a Cartesian coordinate system (x_1, x_2, x_3) as

$$\sum_{i=1}^{3} \frac{\partial \tilde{T}_{x_k x_i}}{\partial x_i} = \rho \frac{\tilde{v}_{x_k}}{\partial t}, \tag{1}$$

$$\tilde{T}_{x_i x_j} = \sum_{l=1}^{3} \sum_{m=1}^{3} \tilde{C}_{x_i x_j x_l x_m} \tilde{S}_{x_l x_m}, \tag{2}$$

where t, ρ, $\tilde{S}_{x_i x_j}$, $\tilde{T}_{x_i x_j}$, $\tilde{v}_{x_i}$, and $\tilde{C}_{x_i x_j x_k x_l}$ are respectively time, mass density, the $x_i x_j$-components of the strain and stress tensors, the x_i-component of the particle velocity, and the $x_i x_j x_k x_l$-component of the stiffness tensor.

We normalize the variables as $T_{x_i x_j} = \tilde{T}_{x_i x_j}/C_N$, $C_{x_i x_j x_l x_m} = \tilde{C}_{x_i x_j x_l x_m}/C_N$, and $v_{x_i} = \tilde{v}_{x_i}/V_N$, where $C_N = \max\{\tilde{C}_{x_i x_j x_k x_l} | i, j, k, l \in \{1, 2, 3\}\}$ and $V_N = \sqrt{C_N/\rho}$. We can rewrite Eq. (1) and the time derivative of Eq. (2) as

$$\sum_{i=1}^{3} \frac{\partial T_{x_k x_i}}{\partial x_i} = \frac{\rho V_N}{C_N} \frac{\partial v_{x_k}}{\partial t}, \tag{3}$$

$$\frac{\partial T_{x_i x_j}}{\partial t} = \sum_{l=1}^{3} \sum_{m=1}^{3} C_{x_i x_j x_l x_m} V_N \frac{\partial v_{x_l}}{\partial x_m}. \tag{4}$$

We consider a two-dimensional $[\partial/\partial x_3 = 0]$ Lamé-mode resonator with a length of $2nb$ and a width of $2ma$ on an anisotropic plate, where m and n are natural numbers, which correspond to the order of Lamé modes. The unit cell of a rectangular SGCV, the length and width of which are respectively Δ_y and Δ_x, is shown in Fig. 1. Hereafter, we will represent x_i $(i = 1, 2)$ as x and y for simplicity.

The Lamé-mode resonator is discretized with the SGCV with a length of Δ_y and a width of Δ_x, as shown in Fig. 2. Here, $N_x = 2ma/\Delta_x$ and $N_y = 2nb/\Delta_y$ are the numbers of cells in the x- and y-directions, respectively. We represent a function of space and time $f(x,y,t)$ on $x = \tilde{I}\Delta_x$, $y = \tilde{J}\Delta_y$, and $t = \tilde{N}\Delta_t$ as $f^{\tilde{N}}(\tilde{I},\tilde{J})$, where $\tilde{I}$, $\tilde{J}$, and $\tilde{N}$ are integer or half-integer numbers. Here, Δ_t is the time interval. We define the Courant number R as $V_N\Delta_t/\Delta$, where $\Delta = \min\{\Delta_x, \Delta_y\}$.

By multiplying the left- and right-hand sides of Eq. (3) by $R\Delta$ and $V_N\Delta_t$, respectively, Eq. (3) is discretized as

$$v_\xi^{N+1}\left(I+\frac{1}{2}, J+\frac{1}{2}\right) - v_\xi^{N}\left(I+\frac{1}{2}, J+\frac{1}{2}\right) = R\Delta\left[\frac{T_{\xi x}^{N+1/2}(I+1, J+\frac{1}{2}) - T_{\xi x}^{N+1/2}(I, J+\frac{1}{2})}{\Delta_x} + \frac{T_{\xi y}^{N+1/2}(I+\frac{1}{2}, J+1) - T_{\xi y}^{N+1/2}(I+\frac{1}{2}, J)}{\Delta_y}\right], \quad (5)$$

where ξ denotes x or y. Here, we note that $\rho V_N^2/C_N = 1$.

To discretize Eq. (4), we consider Eq. (4) for $T_{\xi x}$ ($\xi = x, y$) as an example. By multiplying the left- and right-hand sides of Eq. (4) by Δ_t and $R\Delta/V_N$, respectively, the left-hand side and $\partial v_\xi/\partial x$ on the right-hand side are discretized as

$$\Delta_t \left.\frac{\partial T_{\xi x}}{\partial t}\right|_{(I,J+1/2)}^{N} = T_{\xi x}^{N+1/2}(I, J+1/2) - T_{\xi x}^{N-1/2}(I, J+1/2), \quad (6)$$

$$\frac{R\Delta}{V_N} V_N \left.\frac{\partial v_\xi}{\partial x}\right|_{(I,J+1/2)}^{N} = R\Delta \frac{v_\xi^{N}(I+1/2, J+1/2) - v_\xi^{N}(I-1/2, J+1/2)}{\Delta_x}. \quad (7)$$

The remaining term $\partial v_\xi/\partial y|_{(I,J+1/2)}^{N}$ on the right-hand side of Eq. (4) is evaluated using Eqs. (12)–(18) in the paper of Yasui et al.[18] Equation (4) for $T_{\xi y}$ is also discretized in the same manner.

We consider quartz as the anisotropic plate and use Bechmann's values[21] of $C_{11} = 86.74 \times 10^9$ Nm^{-2}, $C_{12} = 6.99 \times 10^9$ Nm^{-2}, $C_{13} = 11.91 \times 10^9$ Nm^{-2}, $C_{14} = -17.91 \times 10^9$ Nm^{-2}, $C_{33} = 107.2 \times 10^9$ Nm^{-2}, $C_{44} = 57.94 \times 10^9$ Nm^{-2}, and $C_{66} = 39.88 \times 10^9$ Nm^{-2}, where indices are abbreviated. We found that Lamé modes can exist when Euler's angle is (0°, −29.347°, 0°) and $mb/(na) = 0.9763$.[22] Then, the resonant frequency is given as $f_m = [m/(4a)](c/\rho)^{1/2}$. Here, $c = (C'_{11}C'_{22} - C'^2_{12})/(C'_{22} + C'_{12})$, where C'_{ij} $(i, j = 1, 2)$ denotes the stiffness in the above orientation. We note that the piezoelectricity of quartz is not taken into account in our calculation.

For our FD-TD calculations, R, the number of total time steps, N_t, and Δ_y are respectively taken as 0.5, $8000a/\Delta_x$, and $2mb/N_x$ $[N_x/m = N_y/n]$. The x-component of the particle velocity, v_x, is vibrated as a sine-modulated Gaussian pulse given as

$\sin(2\pi f_m t)\exp[-(t-t_0)^2/(2w_0^2)]$ with $t_0 = 2800a\Delta_t/\Delta_x$ and $w_0 = 100a\Delta_t/(\sqrt{2}\Delta_x)$ at a point $(x_0+\Delta_x/2, y_0+\Delta_y/2)$, where $x_0 = \lfloor(N_x/4)\rfloor\Delta_x$ and $y_0 = \lfloor(N_y/4)\rfloor\Delta_y$. The time response of v_x, which is shown in Fig. 3 for the calculation of the fundamental Lamé mode $[m = n = 1]$ as an example, is observed at a point $(3x_0 + \Delta_x/2, 3y_0 + \Delta_y/2)$ to extract the resonant frequency f_{FDTD} by the FFT. Following Yasui et al.[18,19] we use a procedure for the computation of resonance frequencies from time responses at a time interval $[0, N_t\Delta_t]$. We also note that a condition for the Lamé mode, which is given as $T_{xy} = T_{yx} = 0$, is not taken into account in our FD-TD calculations of Eqs. (5) and (6): T_{xy} and T_{yx} are computed in each time step.

Table I shows the normalized resonant frequency f_{FDTD}/f_m values of the fundamental and higher-order modes of the Lamé-mode resonator, where f_{FDTD} denotes the resonant frequency calculated by the proposed method. The error is less than 0.4% for $2a/\Delta_x \geq 20$. We can see very good agreement between the calculated and theoretical values. The normalized resonant frequency f_{FDTD}/f_m values oscillate for varying values of $2a/\Delta_x$ because of the fact that the frequency at the peak in the spectrum and the frequency resolution depend on Δ_t, which is a function of Δ_x.

Figure 4 shows the mode shapes calculated by the proposed method. We can see that the fundamental and higher-order Lamé modes are excited.

In conclusion, the FD-TD method with the rectangular SGCV for anisotropic materials was formulated. The proposed method was applied to resonant frequency analysis for Lamé-mode resonators on a quartz plate. The resonant frequencies of the fundamental and higher-order modes were evaluated and agreed very well with the theoretical values. The consideration of piezoelectricity in our method will be our future work.

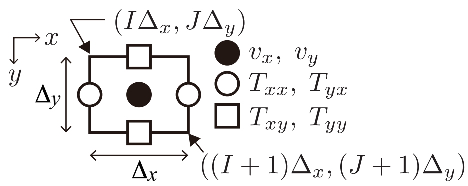

Fig. 1. Unit cell of rectangular SGCV in two dimensions for elastic waves propagating in an anisotropic plate.

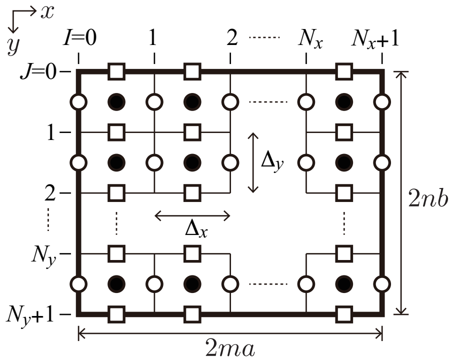

Fig. 2. Lamé-mode resonator discretized with the rectangular SGCV.

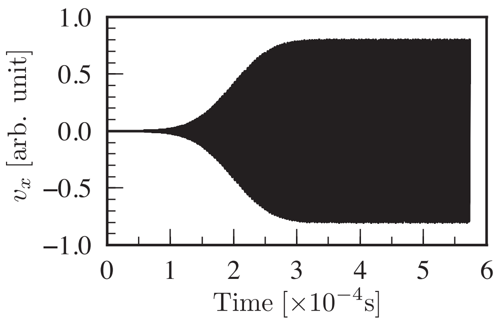

Fig. 3. Time response of the x-component of the particle velocity at the observation points for the calculation of the fundamental Lamé mode.

Table I. Extracted normalized resonant frequency f_{FDTD}/f_m values of the fundamental and higher-order Lamé modes of the Lamé-mode resonator on a quartz plate.

	(m, n)				
$2a/\Delta_x$	$(1, 1)$	$(2, 1)$	$(3, 1)$	$(2, 2)$	$(3, 3)$
20	1.0028	1.0028	1.0028	1.0037	1.0037
50	1.0006	1.0006	1.0006	1.0006	1.0006
100	1.0006	0.9995	1.0006	0.9995	1.0006
150	0.9997	0.9997	0.9997	0.9997	0.9997

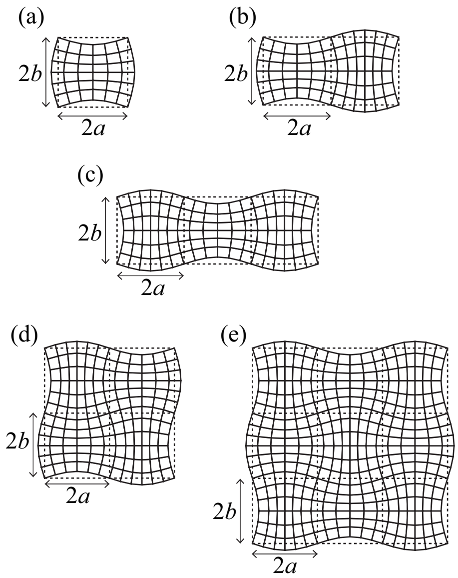

Fig. 4. Mode shapes (solid lines) and cross sections of the resonators (dashed lines) for the fundamental and higher-order modes: (a) $m = 1$, $n = 1$, (b) $m = 2$, $n = 1$, (c) $m = 3$, $n = 1$, (d) $m = 2$, $n = 2$, and (e) $m = 3$, $n = 3$.

References

1) T. Yiyu, Y. Inoguchi, Y. Sato, M. Otani, Y. Iwaya, H. Matsuoka, and T. Tsuchiya, Jpn. J. Appl. Phys. **53**, 07KC14 (2014).
2) S. Maruo and A. Hosokawa, Jpn. J. Appl. Phys. **53**, 07KF06 (2014).
3) S. Tanaka, K. Shimizu, S. Sakuma, T. Tsuchiya, and N. Endoh, Jpn. J. Appl. Phys. **52**, 07HF09 (2013).
4) A. Hosokawa, Jpn. J. Appl. Phys. **53**, 07KF13 (2014).
5) O. Yamashita, T. Tsuchiya, Y. Iwaya, M. Otani, and Y. Inoguchi, Jpn. J. Appl. Phys. **54**, 07HC02 (2015).
6) K. Shimizu, T. Tsuchiya, K. Fukasawa, Y. Hatano, and N. Endoh, Jpn. J. Appl. Phys. **54**, 07HF22 (2015).
7) A. Sugawara, K. Jinno, Y. Ohara, and K. Yamanaka, Jpn. J. Appl. Phys. **54**, 07HC08 (2015).
8) A. Hosokawa, Jpn. J. Appl. Phys. **54**, 07HF06 (2015).
9) J. Virieux, Geophysics **51**, 889 (1986).
10) A. Levander, Geophysics **53**, 1425 (1988).
11) E. H. Saenger, N. Gold, and S. A. Shapiro, Wave Motion **31**, 77 (2000).
12) T. Bohlen and E. H. Saenger, Geophysics **71**, T109 (2006).
13) M. Sato, Jpn. J. Appl. Phys. **44**, 4490 (2005).
14) V. I. Lebedev, USSR Comput. Math. Math. Phys. **4**, 69 (1964).
15) V. Lisitsa and D. Vishnevskiy, Geophys. Prospect. **58**, 619 (2010).
16) H. Bernth and C. Chapman, Geophysics **76**, WA43 (2011).
17) K. Hasegawa and T. Shimada, Jpn. J. Appl. Phys. **51**, 07GB04 (2012).
18) T. Yasui, K. Hasegawa, and K. Hirayama, Jpn. J. Appl. Phys. **52**, 07HD07 (2013).
19) T. Yasui, K. Hasegawa, and K. Hirayama, Jpn. J. Appl. Phys. **54**, 07HD04 (2015).
20) T. Yasui, K. Hasegawa, and K. Hirayama, Proc. 36th Symp. Ultrasonic Electronics, 2015, 3J2-1.
21) R. Bechmann, A. D. Ballato, and T. J. Lukaszek, Proc. IRE **50**, 1812 (1962).
22) R. D. Mindlin, J. Appl. Phys. **27**, 1462 (1956).